Current Biology, Vol. 14, 314–321, February 17, 2004, ©2004 Elsevier Science Ltd. All rights reserved. DOI 10.1016/j.cub.2004.01.052

nanos and *pumilio* Are Essential for Dendrite Morphogenesis in *Drosophila* Peripheral Neurons

Bing Ye,[1] Claudia Petritsch,[1] Ira E. Clark,[2] Elizabeth R. Gavis,[2] Lily Yeh Jan,[1] and Yuh Nung Jan[1,*]

[1]Howard Hughes Medical Institute
Department of Physiology
Department of Biochemistry and Biophysics
University of California, San Francisco
San Francisco, CA 94143-0725

[2]Department of Molecular Biology
Princeton University
Princeton, NJ 08544

Summary

Much attention has focused on dendritic translational regulation of neuronal signaling and plasticity [1, 2]. For example, long-term memory in adult *Drosophila* requires Pumilio (Pum) [3], an RNA binding protein that interacts with the RNA binding protein Nanos (Nos) to form a localized translation repression complex essential for anterior-posterior body patterning in early embryogenesis [4]. Whether dendrite morphogenesis requires similar translational regulation is unknown. Here we report that *nos* and *pum* control the elaboration of high-order dendritic branches of class III and IV, but not class I and II, dendritic arborization (da) neurons. Analogous to their function in body patterning, *nos* and *pum* require each other to control dendrite morphogenesis, a process likely to involve translational regulation of *nos* itself. The control of dendrite morphogenesis by Nos/Pum, however, does not require *hunchback*, which is essential for body patterning. Interestingly, Nos protein is localized to RNA granules in the dendrites of da neurons, raising the possibility that the Nos/Pum translation repression complex operates in dendrites. This work serves as an entry point for future studies of dendritic translational control of dendrite morphogenesis.

Results and Discussion

Expression of Nos and Pum in Dendritic Arborization Neurons

Early in *Drosophila* embryogenesis, Nos protein is first detected in the posterior end of the embryo and then in the pole cells [5], whereas Pum protein is uniformly distributed [6]. Characterization of later expression has been limited to the ovary for Nos [7] and to the adult head for Pum [3, 8]. Several recent findings implicate Nos and Pum in eye development [9], optic nerve development [10], neuronal excitability [8], and long-term memory [3]. To determine whether Nos and Pum regulate dendrite morphogenesis, we examined their expression and function in the dendritic arborization (da) neurons in the *Drosophila* peripheral nervous system (PNS).

*Correspondence: ynjan@itsa.ucsf.edu

The da neurons [11] have proven to be useful for studies of dendrite development [12–17]. The 15 da neurons in each hemisegment of larvae fall into four classes, class I, II, III, and IV, with increasing complexity of dendritic morphology [15]. The highest order dendrites of class I and II da neurons are fourth-order dendrites. Most of the terminal branches of class III neurons are fifth-order dendrites with a distinctive structure referred to as dendritic spikes [15]. The class IV neurons have highly branched dendrites with terminal branches typically above the fifth-order.

Nos and Pum were expressed in all da neurons (Figures 1A and 1B), as revealed by immunocytochemistry with antibodies against Nos or Pum in third-instar larvae from a transgenic line carrying GFP marker 80G2, which marks all da neurons [12]. Neuronal expression of *nos* was further confirmed with two independent GAL4 drivers under the control of the *nos* promoter, P{*GAL4-nos*.NGT}40 [18] and *nos*-GAL4::VP16 [19]. We observed mCD8-GFP immunoreactivity in da neurons (Figure 1C) of larvae that carried both P{*GAL4-nos*.NGT}40 and a reporter gene, *UAS-mCD8-GFP*, suggesting that the *nos* promoter is active in da neurons. Similar neuron-specific expression was also observed with *nos*-GAL4::VP16, which was inserted into a different chromosome and yielded some segment-to-segment variations in the expression pattern.

nos and *pum* Are Essential for the Morphogenesis of High-Order Dendritic Branches

Overexpression of *nos-tub3′UTR* in class III and class IV neurons (Figures 2E and 2H), but not class I neurons (Figure 2B), dramatically changed dendrite morphology compared with the control (Figures 2A, 2D, and 2G), in which only the reporter gene *UAS-mCD8-GFP* was overexpressed. In both class III and class IV neurons, the number of high-order dendritic branches was significantly reduced while the morphology of the major branches was not affected. Overexpressing *pum* caused a similar change specific to dendrites of class III and IV neurons (Figures 2F and 2I). Neither the dendrites of bipolar neurons nor those of chordotonal neurons were affected by overexpressing *nos* or *pum* (data not shown).

The loss of function phenotype of *nos* and *pum* in dendrite morphogenesis was assessed via mosaic analysis with a repressible cell marker (MARCM) [20]. The MARCM system provides an effective way to study every type of PNS neuron, including da neurons, chordotonal neurons, bipolar neurons, and external sensory (es) neurons, with single cell resolution. We could therefore determine which of these neurons were affected by *nos* or *pum* mutation. In addition, by specifically eliminating *nos* or *pum* function in da neurons, we could determine whether these genes act cell-autonomously in dendritic morphogenesis. As a control, MARCM analysis was performed with a chromosome carrying an unrelated transgene.

Loss of *nos* or *pum* in class I or II da neurons did not

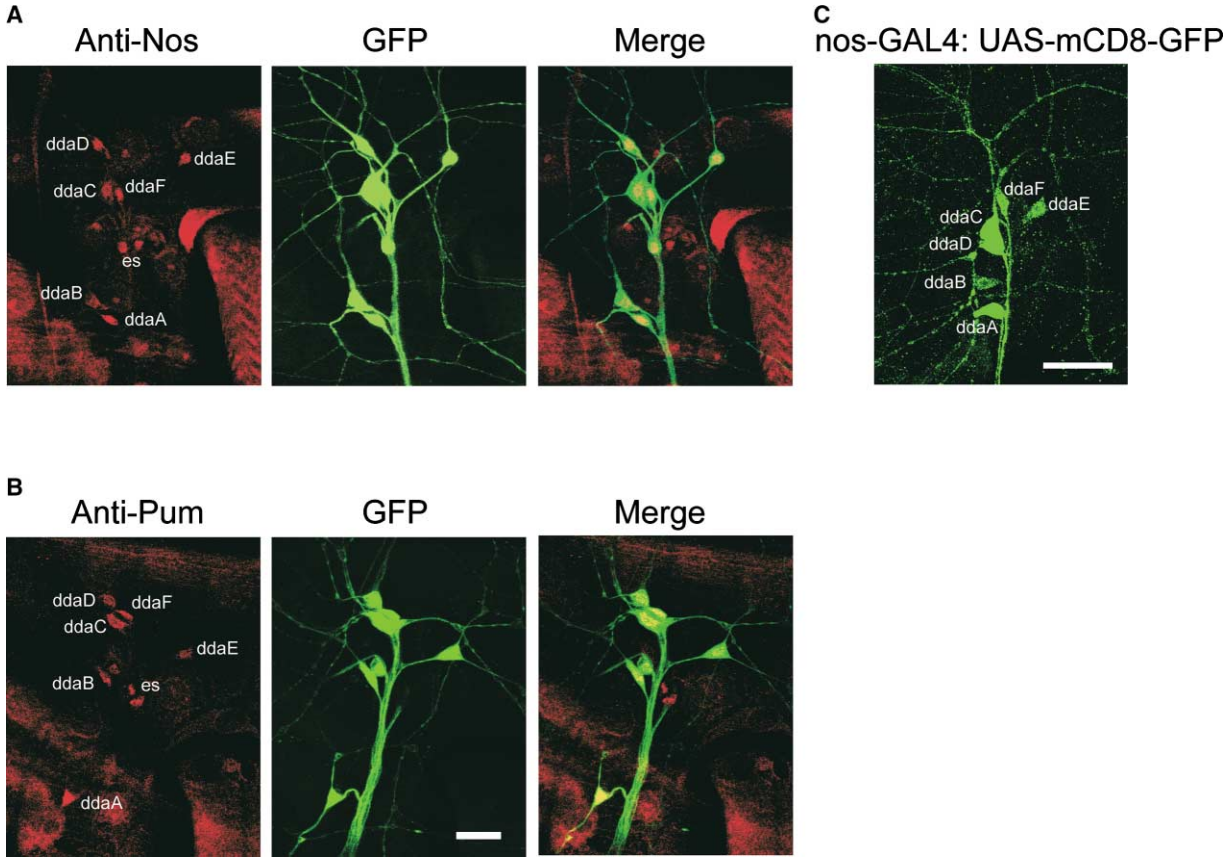

Figure 1. Expression of Nos and Pum in Dendritic Arborization Neurons of the Dorsal Cluster

(A and B) Third-instar larvae carrying the 80G2 GFP marker for da neurons were stained with anti-Nos (A) or anti-Pum (B). Neurons are marked by GFP fluorescence (middle panel).

(C) Immunostaining of the reporter mCD8 driven by P{*GAL4-nos*.NGT}40, a GAL4 driver fused to the *nos* promoter, reveals the *nos* expression pattern. The scale bar represents 20 μm.

alter dendrite morphology (data not shown), as assessed from the total length of dendrites (Figure 3H) and quantitation of dendritic order (Figure 3I). In contrast, in class III neurons lacking *nos* or *pum* function, the characteristic dendritic spikes were significantly elongated (Figures 3A, 3B, and 3C), but the order of dendrites and the length of major dendritic branches (all dendrites except dendritic spikes) were indistinguishable from those of wild-type neurons. Whereas around 2%–10% of dendritic spikes of wild-type ddaA neurons are longer than 10 μm, loss of *nos* or *pum* function caused about 10%–30% of spikes to be longer than 10 μm in about 50% of ddaA neurons (Figure 3D).

Class IV neurons deficient for *nos* or *pum* function also exhibited abnormality in their dendrites. The dendrites of wild-type class IV neurons cover the epidermis in a complete but nonoverlapping fashion and thereby "tile" the body wall [15] (Figure 3E). Incomplete coverage of the epidermis was observed in 20% of neurons mutant for *nos* (3 in 15) (Figure 3F) and about 15% of those mutant for *pum* (4 in 26) (Figure 3G) as a result of the reduction of higher-order branches. Therefore, both *nos* and *pum* are required for the proper morphogenesis of dendrites, especially the high-order dendritic branches, in a cell type-specific manner.

nos and *pum* Act Together in Dendrite Morphogenesis

Given the similar dendrite phenotypes of *nos* and *pum* mutants, we wondered whether there is a mutual requirement of *nos* and *pum* for dendrite morphogenesis, as in embryogenesis [21]. We first tested whether *pum* function is required for *nos* overexpression to eliminate high-order dendritic branches in class IV neurons. Indeed, when *nos* was overexpressed in a *pum* null background (Figure 4A, part c), the high-order dendritic branches were not as drastically reduced as those in the case of *nos* overexpression in a wild-type background (Figure 4A, part b). We then reasoned that, if *nos* and *pum* require each other in regulating dendrite morphogenesis, the dendrite phenotypes of *pum, nos* double mutants should resemble those of single mutants of *nos* or *pum*. We employed MARCM analysis to examine the dendrites of da neurons mutant for both *nos* and *pum*. Eliminating both *nos* and *pum* functions in class I da neurons did not result in any defect in dendrite morphology (Figures 4B, part a, 3H, and 3I). The number of long dendritic spikes in class III neurons was increased (Figure 4B, part b) to a similar extent as in the *nos* and *pum* single mutants (Figure 3D). Moreover, we also observed incomplete innervation of the territory in 18% of neurons mutant for both *nos* and *pum* (5 in 28 clones),

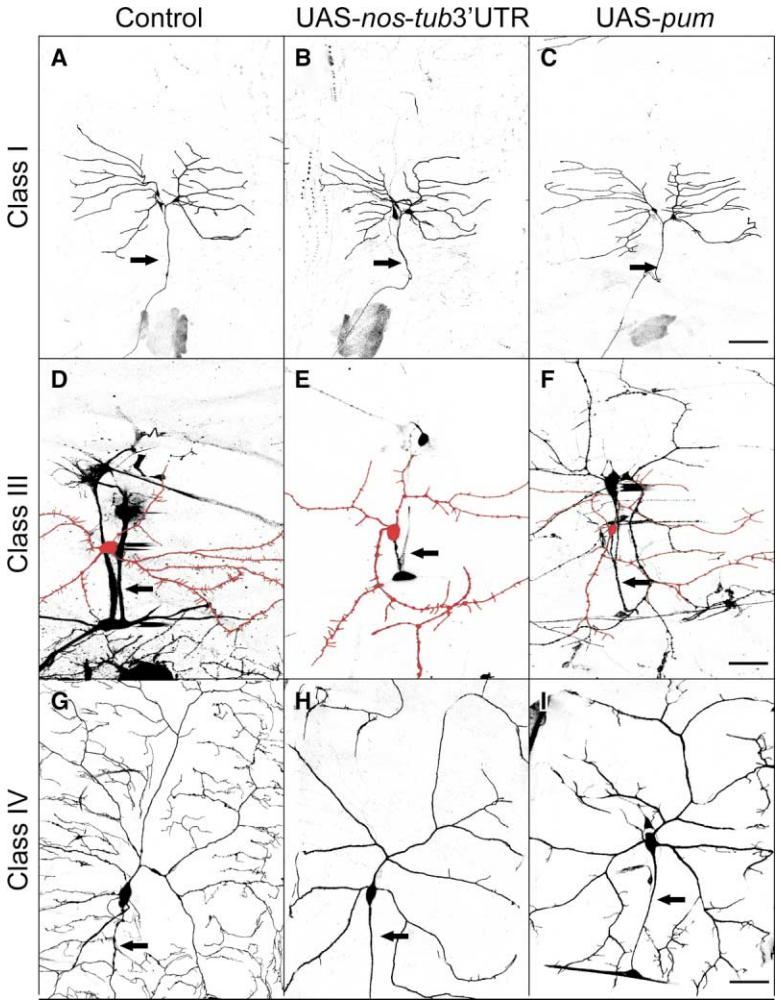

Figure 2. Overexpression of *nos* and *pum* Results in Reduction of High-Order Dendritic Branches in Class III and IV, but Not Class I, Dendritic Arborization Neurons

The GAL4/UAS system was used to express *nos* or *pum* along with the reporter *UAS-mCD8-GFP* in class I ($GAL4^{2-21}$), III ($GAL4^{109(2)80}$ or $GAL4^{5-78}$), or IV ($GAL4^{4-77}$) da neurons. To avoid potential translational repression mediated by the TCE within the 3′UTR of *nos* mRNA [30], we replaced the *nos* 3′UTR by α-*tubulin3′UTR* sequences [24]. As the control, *UAS-mCD8-GFP* alone was overexpressed with these GAL4 drivers.

(A–C) Class I da neurons ddaD and ddaE. ddaE projects lateral dendrites anteriorly, whereas ddaE projects lateral dendrites posteriorly.

(D–F) Class III da neurons ddaA (highlighted in red). Without a GAL4 driver specific for class III neurons, we overexpressed *nos-tub3′UTR* with a general da neuron driver $GAL4^{109(2)80}$ and then ablated the adjacent neurons with laser beams to examine the gain of function of *nos* with high resolution (E). In the control experiment, we used the same driver to express just the *UAS-mCD8-GFP* reporter gene (D). To avoid lethality as a result of expressing *pum* with driver $GAL4^{109(2)80}$, we used $GAL4^{5-78}$ to drive expression in class I, III, and IV da neurons without laser ablation of adjacent neurons (F). Note that there is a decrease in the number of dendritic spikes when *nos-tub3′UTR* or *pum* is overexpressed in class III neurons.

(G–I) Class IV da neuron ddaC. Arrows point to the axons of the da neurons. The scale bar in (A)–(C) represents 80 μm, and that in (D)–(I) represents 40 μm.

an extent similar to that in the single mutant of either *nos* (20%) or *pum* (15%), as a result of reduced numbers of high-order branches in class IV neurons (Figure 4B, part c). Taken together, these data indicate that *nos* and *pum* require each other to regulate dendrite morphology, possibly by forming a protein complex as they do in embryogenesis.

Pum-Homology Domain Is Sufficient for the Gain of Function of Pumilio

The only domain structure identified so far in Pum protein is the so-called "Pumilio-homology domain" (Pum-HD), which consists of eight repeats of 36 amino acids and is conserved in various species, including humans. Pum-HD is responsible for binding to the *nos* response elements (NRE's) of *hb* mRNA [9], as well as Nos [22], and is sufficient for Pum function in embryogenesis [9]. To investigate whether this RNA binding domain is sufficient for dendrite morphogenesis, we overexpressed Pum-HD in class IV da neurons. Overexpression of Pum-HD virtually replicated the dendrite phenotype that had been produced by overexpression of full-length Pum (Figure 5A). Therefore, it is likely that the Nos/Pum complex regulates the downstream molecules through the RNA binding domain of Pum.

hunchback Is Not Required for the Control of Dendrite Morphogenesis by the Nos/Pum Complex

The major target mRNA of the Nos/Pum translational repression complex in anterior-posterior body patterning is the *hb* mRNA, which binds to Pum through the NRE's in its 3′ UTR. A single amino acid change in Pum, Glycine[1330] to Aspartate (Pum^{G1330D}), renders Pum defective in the suppression of *hb* translation. However, Pum^{G1330D} still binds RNA and recruits Nos into the Nos/Pum/*hb* mRNA complex. We overexpressed this mutant *pum* in class IV da neurons and found that pum^{G1330D}, like wild-type *pum*, reduced high-order dendritic branches (Figure 5A). This result suggests that *hb* is not essential for the Nos/Pum translational control complex to regulate dendrite morphogenesis. Consistent with this finding, immunocytochemistry revealed no Hb protein in larval da neurons (data not shown). Moreover, no defect in dendrite morphology was observed in any of the four classes of da neurons in loss of *hb* function MARCM clones (Figures 3D, 3H, and 3I). Taken together, these observations indicate that the Nos/Pum complex regulates RNA targets other than *hb* mRNA in da neurons.

If we are to fully understand the roles of Nos and Pum in dendrite morphogenesis, it is crucial to identify the RNA targets of this complex in dendrites. The dendrite phenotypes described here provide a guide for search-

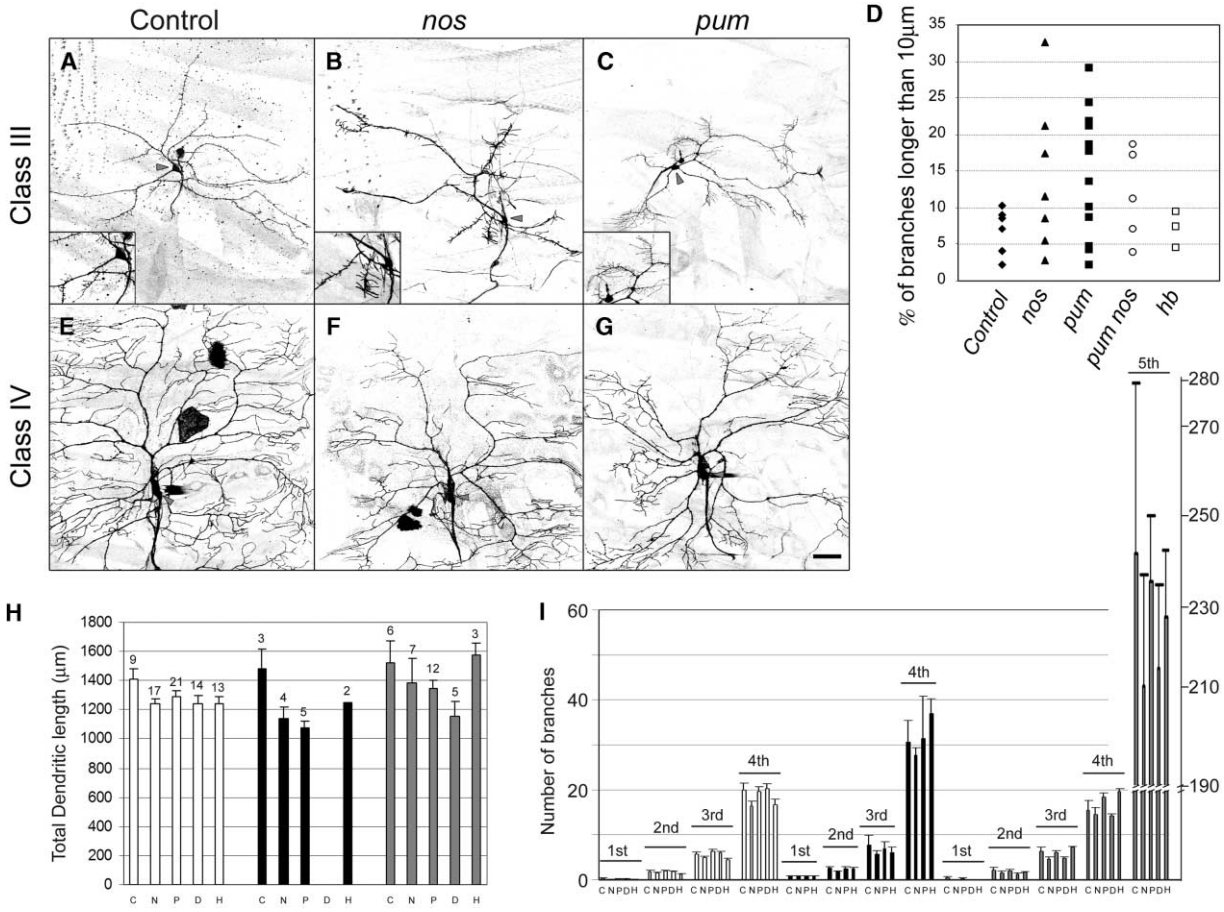

Figure 3. Class III and IV Neurons Lacking *nos* or *pum* Exhibit Abnormality in Dendrite Morphology

(A–C) Mosaic clones of class III da neuron ddaA. The insets in (A)–(C) show magnified images of parts of the class III neurons with characteristic dendritic spikes. Note that in *nos* (B) and *pum* (C) mutant neurons, many dendritic spikes are longer than those in wild-type neurons (A).

(D) Percentage of dendritic spikes that are longer than 10 μm in the class III da neuron ddaA homozygous for control (solid diamond), *nos* (solid triangle), *pum* (solid square), *pum nos* (empty circle), and *hb* (empty square). Each symbol represents the percentage in one ddaA mosaic clone.

(E–G) Mosaic clones of class IV da neuron ddaC. Note that there are areas devoid of ddaC dendrites in the body wall of *nos* (F) and *pum* (G) mutant neurons, whereas this dorsal part of the body wall is covered by the dendrites of wild-type ddaC (E). Cell bodies of the neurons are marked with gray arrowheads. The scale bar represents 40 μm.

(H) Total length of all dendrites of class I (white bars) and II (black bars) and that of the major branches (all dendrites except dendritic spikes) of class III da neurons (gray bars). Values shown in the graph are mean ± standard error of the mean. Numbers of samples (n) are indicated on top of each bar. There is no significant difference ($p > 0.05$) between major dendritic branches of *nos* (N), *pum* (P), *pum nos* (D), or *hb* (H) mutant neurons and control (C) neurons in any of these classes of neurons (Student's t test)

(I) Numbers of dendritic branches in each order, as revealed by reversed Strahler analysis [15, 31, 32]. Values are mean ± standard error. Data on Class I neurons (white bars) were collected from ddaD and ddaE. Sample size: control (C) = 10, *nos* (N) = 17, *pum* (P) = 19, *pum nos* (D) = 12, and *hb* (H) = 13. Data on class II neurons (black bars) were from ddaB. Sample size: control (C) = 3, *nos* (N) = 3, *pum* (P) = 5, *pum nos* (D) = 0, and *hb* (H) = 2. Data on class III neurons (gray bars) were from ddaA. Sample size: control (C) = 6, *nos* (N) = 7, *pum* (P) = 12, *pum nos* (D) = 5, and *hb* (H) = 3. All of these neurons are in the dorsal cluster. There is no significant difference ($p > 0.05$) between *nos*, *pum, pum nos,* or *hb* and the control, in dendritic orders in any of the three classes of da neurons, as indicated by the t test.

ing for the RNA targets of the Nos/Pum complex in our ongoing genetic screen for dendrite development. Moreover, the epitope-tagged Pum RNA binding domain, which is sufficient for Pum function in dendrites (Figure 5B), will be a useful tool for biochemically identifying the RNA targets.

Nos Protein Is Localized to RNA Granules in Dendrites

To elucidate the possible site of Nos/Pum action, we studied the subcellular distribution of Nos. Because the anti-Nos antibody also stains muscle in larvae (Figure 1), it was difficult to examine Nos distribution in neuronal processes situated near muscle. To circumvent this technical problem, we generated a transgene of Nos fused to an HA-epitope tag at the N terminus and expressed it in da neurons, but not muscles, by using the GAL4/UAS binary system. HA-Nos is localized to distinctively punctuate structures in both soma and dendrites (Figure 5B). These structures are round and uniform in size, with a diameter of around 0.3 μm, which is reminiscent of the RNA granules ranging from 0.175–0.6 μm in diameter in mammalian cortical neurons [23]. We then double stained the larval preparation with both

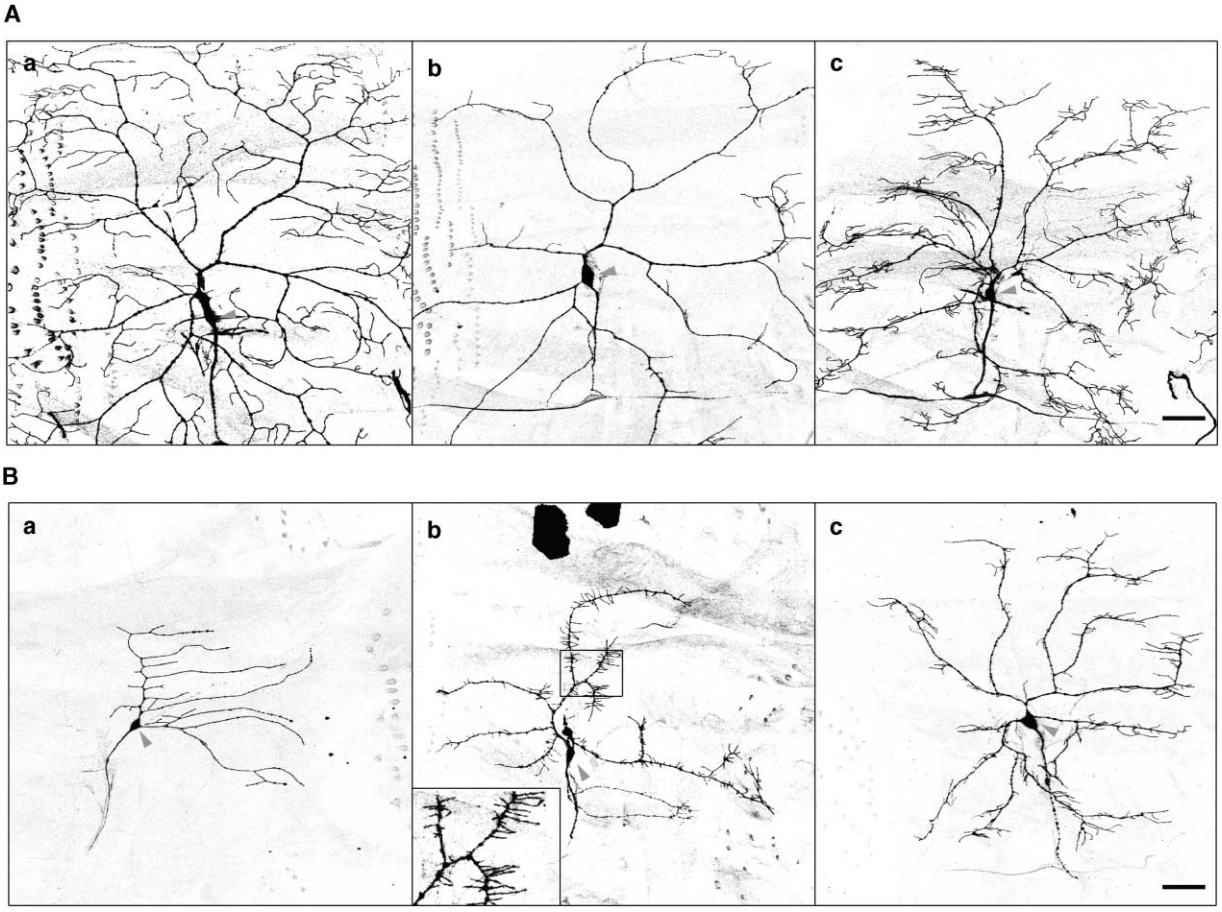

Figure 4. *nos* and *pum* Act Together to Regulate Dendrite Morphogenesis

(A) *nos* requires *pum* to regulate dendrite morphogenesis. (a) Control. The reporter gene *UAS-mCD8-GFP* was expressed in class IV da neuron ddaC with $GAL4^{4-77}$. (b) UAS-*nos tub3′UTR* was overexpressed in ddaC with $GAL4^{4-77}$. (c) UAS-*nos tub3′UTR* was overexpressed in ddaC in pum^{ET1}/pum^{ET1} larvae.

(B) *nos* and *pum* require each other to regulate dendrite morphology. The effects of missing both *nos* and *pum* on dendrite morphology was analyzed with MARCM. (a) class I da neuron ddaE; (b) class III da neuron ddaA; (c) class IV da neuron ddaC. The cell bodies are marked with arrowheads. The scale bar represents 40 μm.

anti-HA antibody and Syto 14, a nucleic acid dye that preferentially labels RNA [23], and found that Nos colocalizes with RNA granules (Figure 5B).

Regulation of *nos* Function in Dendritic Arborization Neurons by a Translational Control Element

Essential for the posteriorly localized translation repression of *hb* by Nos/Pum complex, translation of Nos itself is repressed in the anterior of the embryo via a 90 nucleotide translational control element (TCE) located in the 3′ untranslated region (3′UTR) of *nos* mRNA. In a subset of *Drosophila* central neurons, ectopic expression of *nos* causes the wing expansion phenotype only upon replacement of the TCE-bearing 3′UTR with α-*tubulin (tub) 3′UTR* (*nos-tub3′UTR*), thereby removing the TCE-dependent translational suppression of the *nos* transgene [24]. To examine whether a mechanism analogous to that for the translational repression of *nos* in the embryo exists in da neurons, we used a GAL4 driver ($GAL4^{8-123}$) to ectopically express *nos-tub3′UTR* mRNA inserted with the *nos* TCE (*nos-tub:nos+2*) [24]. The *nos-tub3′UTR* and *nos-tub:nos+2* transgenes have been shown to have little position effect in expression [24]. Overexpression of *nos-tub3′UTR* resulted in reduction of the amount of high-order dendritic branches, a dendrite phenotype similar to that produced by $GAL4^{4-77}$ (Figures 5C and 5D). Overexpression of *nos-tub:nos+2* with $GAL4^{8-123}$ significantly reduced the severity of the phenotype (Figure 5C and 5D), thereby suggesting the presence of a mechanism for translational repression of *nos* in class IV da neurons.

Both *nos* and *pum* genes are conserved in various species, including mammals. Two *nos* genes have been identified in humans [22], and three have been identified in mice [25, 26]. The zygotic *nos1* is highly expressed in the nervous system but not in developing germ cells [25]. It is unclear whether *nos2* and *3* are expressed in the nervous system [26]. There have been no gross anatomical defects observed in mice deficient for *nos1* [25]. In light of our study, it would be of interest to conduct a detailed investigation on neuron morphology with single-cell resolution to ascertain whether these mice exhibit any defects in dendrite morphology, especially of high-order dendritic branches. It is also impor-

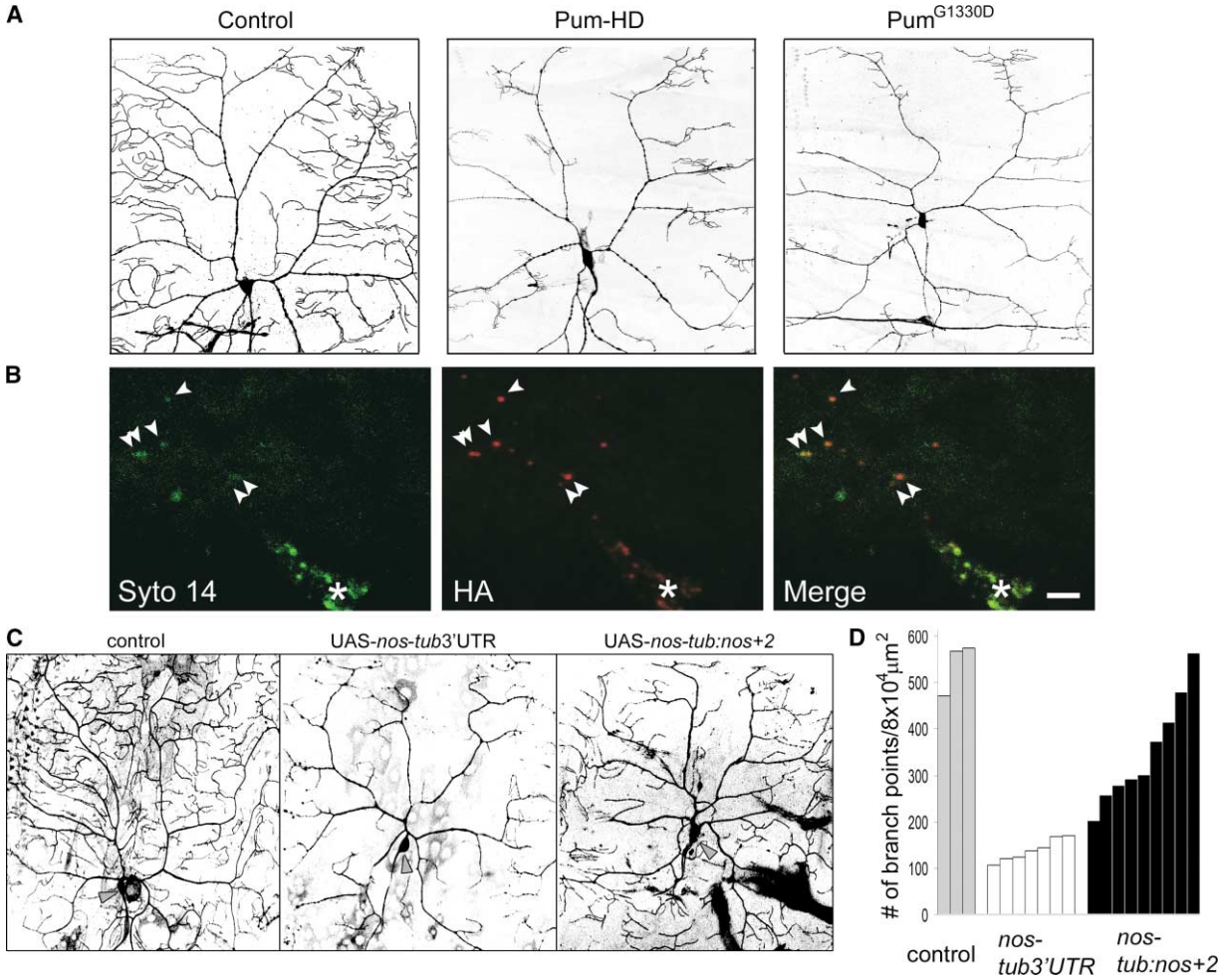

Figure 5. Mechanism of the Regulation of Dendrite Morphogenesis by the Nos/Pum Complex

(A) The RNA binding and Nos binding domain of Pum (Pum-HD) is sufficient for Pum function. In the control (left panel), only the marker *UAS-mCD8-GFP* was expressed in class IV da neuron ddaC with $GAL4^{4-77}$. Overexpression of the Pum homology domain (Pum-HD) was sufficient to reduce high-order dendritic branches in class IV da neurons (middle panel). Overexpression of Pum^{G1330D}, which is incapable of repressing *hb* translation, reduced high-order dendritic branches in ddaC (right panel). Compare with Figure 2I.

(B) Localization of Nos in RNA granules. $GAL4^{4-77}$ was used for driving both UAS-HA-*nos-tub3′UTR* and *UAS-mCD8-GFP*. Larval fillets were double stained with Syto 14 to reveal RNA granules and with anti-HA antibody to reveal the localization of Nos. Arrowheads indicate the position of granules that contain both RNA and Nos in dendrites. The soma is marked with an asterisk. The scale bar represents 2 μm.

(C) The *nos* translational control element suppresses the *nos* overexpression dendrite phenotype. Note that overexpression of *nos-tub3′UTR* in class IV da neuron ddaC by $GAL4^{8-123}$ resulted in reduction of high-order dendritic branches, and the presence of the *nos* TCE (UAS-*nos-tub:nos+2*) significantly reduced the phenotype. The UAS-*nos-tub:nos+2* line has been previously described [24].

(D) Quantitation of the effects of *nos* overexpression in the absence (*nos-tub3′UTR*) and presence (*nos-tub:nos+2*) of the TCE. Each bar represents the total number of branch points of one ddaC neuron in an 8×10^4 μm^2 area that covers the entire dendritic tree except for narrow areas near the segmental borders. Differences due to the presence or absence of TCE was demonstrable when low expression levels were achieved at 18°C with $GAL4^{8-123}$, rather than $GAL4^{4-77}$, to drive expression in class IV da neurons. The soma of neurons are marked with arrowheads.

tant to determine whether *nos2* and *nos3* are expressed in the nervous system and if their functions are redundant to those of *nos1*. Two *pum* genes, *pum1* and *pum2*, have been cloned in both mice and humans [22, 27]; both genes are expressed in the brain [27]. It will be interesting to see whether these genes take on separate or redundant roles in neurodevelopment and long-term memory, both functions of the *pum* gene in *Drosophila*.

In summary, we have shown that *nos* and *pum* are essential for proper dendrite morphogenesis in subsets of *Drosophila* PNS neurons, and we have provided evidence suggesting that they act by forming a translation control complex, possibly in dendrites. This study could serve as a starting point for future identification and characterization of molecules regulating local translation in both *Drosophila* and mammalian dendrites.

Experimental Procedures

Staining of Larval PNS

Third-instar larvae were dissected for fillet preparations. The fillets were fixed with 4% formaldehyde/1× PBS, permeabilized with 0.3% Triton X-100/1× PBS (wash solution), and then incubated in the blocking solution (5% normal donkey serum/0.3% Triton X-100/1× PBS). Subsequently, the samples were incubated with the primary

antibodies at 4°C overnight, extensively washed with the wash solution, and then incubated with the fluorophore-crosslinked secondary antibodies at 4°C overnight. After extensive washing, the samples were mounted with DPX mountant (Electron Microscopy Sciences, PA). The samples were imaged for fluorescence with a Leica TCS SP2 confocal microscope. The antibodies and dilutions used in this study were rat anti-Nos (1:100), rabbit anti-Pum (1:400) (both were gifts from Dr. R.P. Wharton), rat anti-mCD8 (1:100), mouse anti-22C10 (1:200-1000), and rat anti-HA (1: 200) (clone 3F10, Roche, New Jersey).

For Syto 14 staining, dissected larval fillets were incubated with 100 nM Syto 14 (Molecular Probes, OR) in 1× PBS at 30°C for 20 min before fixation. After that, the procedure was the same as for immunostaining, except that 1% BSA, instead of normal donkey serum, was used as the blocking reagent. Anti-HA antibody was used for staining HA-Nos-containing granules. For confocal microscopy, Syto 14 was excited with a laser with a 488 nm wavelength. Adjusting the sampling wavelength to 500–540 nm avoided overlap with the fluorescent emission of RRX, the fluorophore for the anti-HA staining.

The images of stained samples in this paper are oriented so that dorsal is up and anterior is left.

Generation of Transgenic Lines

For generation of UAS-*pum* lines, *pum* cDNA [28] from pNB40/R7-1 (a gift from R. Lehmann) was subcloned into the Sac I/Xba I site of pSP64 (Promega), excised with EcoR I and Xba I, and introduced into vector pUAST. To generate the pUAST-*pum-HD* line, the cDNA fragment encoding amino acids 1092–1427 was generated by PCR, fused to a V5 tag (Invitrogen, California), and then inserted into pUAST. For generation of pUAST- pum^{G1330D} lines, full-length *pum* was subcloned into vector pSL1190, followed by site-directed mutagenesis to generate the G1330D mutation. The pum^{G1330D} cDNA was then transferred into pUAST. For generation of transgenic flies, the UAS-constructs were injected into w^{1118} embryos, together with a DNA construct encoding the transposase Δ2-3 [29].

MARCM Analysis

For generation of the FRT^{82B} nos^{RC} line, nos^{RC} (91F1 in cytogenetic map) was recombined with FRT^{82B} by crossing nos^{RC} with FRT^{82B} Dl^{9P39}, which carries a dominant allele of *Delta* (91F12-92A1), and then progenies were selected on food containing 0.67 mg/ml G418 for FRT^{82B}. The recombination event was monitored by examination of the loss of the dominant wing phenotype of *Delta* in the progeny. The putative FRT^{82B} nos^{RC} flies were crossed with Df D1 (FX1), which contained a deficiency that uncovers the *nos* gene, and testing the progeny FRT^{82B} nos^{RC}/Df D1 (FX1) females for sterility verified the presence of nos^{RC} alleles.

For generation of the FRT^{82B} pum^{ET1} nos^{RC} line for double mutant study, recombinant flies between FRT^{82B} pum^{ET1} and nos^{RC} were selected by testing for sterility with pum^{2003} and Df D1 (FX1), respectively.

The FRT^{82B} hb^{B1} line was generated by replacement of the ato^{3} allele in a FRT^{82B} ato^{3} line with hb^{B1} allele with an approach similar to that used to generate the FRT^{82B} nos^{RC} line.

For generation of genetic mosaic clones, FRT^{82B} mutant flies were mated with *elav*-GAL4, *UAS-mCD8-GFP*, *hs*-FLP; FRT^{82B} GAL80. After 2 hr of egg collection, the eggs were allowed to develop for 3 hr before heat shock. Two periods of heat shock, 30 min and 45 min, respectively, were carried out with a 30 min interval in between. The eggs were then kept in 25°C until they developed into third-instar larvae [15]. Mosaic clones were preselected from third-instar larvae that displayed GFP fluorescence in the PNS when placed under a fluorescence microscope. The larvae were subsequently dissected for the creation of fillets for immunostaining.

The pan-neuronal marker 22C10 was used to reveal the cell body positions, which helps to identify neurons. Only clones in abdominal segment 2-6 were imaged and quantified to ensure consistency [15].

Acknowledgments

We thank Dr. Ulrike Heberlein and her lab for access to a collection of GAL4 enhancer trap lines, Dr. Wesley Grueber for $GAL4^{4-77}$ and $GAL4^{5-78}$, Daniel Cox for $GAL4^{2-21}$ lines, Dr. Haifan Lin for FRT^{82B} pum^{ET1}, Dr. Robin P. Wharton for anti-Nos and anti-Pum antibodies, Drs. A. Nakamura and K. Hanyu-Nakamura for anti-Nos antibody, Dr. C. Alonso for anti-Hunchback antibody, Dr. Ruth Lehmann for *pum* cDNA, and Dr. Susan Younger for helping with fly genetics. This work was supported by a National Institutes of Health grant (NIH 1R01 NS 40929-0) given to Y.N.J., as well as a National Institutes of Health postdoctoral training grant (T32 NS007-067-24) and a National Research Service Award (1 F32 NS46847-01) given to B.Y. Additionally, E.R.G. is the recipient of a Beckman Young Investigator award. L.Y.J. and Y.N.J. are investigators of the Howard Hughes Medical Institute.

Received: March 24, 2003
Revised: October 15, 2003
Accepted: December 30, 2003
Published: February 17, 2004

References

1. Steward, O., and Schuman, E.M. (2001). Protein synthesis at synaptic sites on dendrites. Annu. Rev. Neurosci. *24*, 299–325.
2. Tang, S.J., and Schuman, E.M. (2002). Protein synthesis in the dendrite. Philos. Trans. R. Soc. Lond. B Biol. Sci. *357*, 521–529.
3. Dubnau, J., Chiang, A.S., Grady, L., Barditch, J., Gossweiler, S., McNeil, J., Smith, P., Buldoc, F., Scott, R., Certa, U., et al. (2003). The staufen/pumilio pathway is involved in *Drosophila* long-term memory. Curr. Biol. *13*, 286–296.
4. Johnstone, O., and Lasko, P. (2001). Translational regulation and RNA localization in Drosophila oocytes and embryos. Annu. Rev. Genet. *35*, 365–406.
5. Wang, C., and Lehmann, R. (1991). Nanos is the localized posterior determinant in Drosophila. Cell *66*, 637–647.
6. Macdonald, P.M. (1992). The Drosophila pumilio gene: an unusually long transcription unit and an unusual protein. Development *114*, 221–232.
7. Wang, C., Dickinson, L.K., and Lehmann, R. (1994). Genetics of nanos localization in Drosophila. Dev. Dyn. *199*, 103–115.
8. Schweers, B.A., Walters, K.J., and Stern, M. (2002). The Drosophila melanogaster translational repressor pumilio regulates neuronal excitability. Genetics *161*, 1177–1185.
9. Wharton, R.P., Sonoda, J., Lee, T., Patterson, M., and Murata, Y. (1998). The Pumilio RNA-binding domain is also a translational regulator. Mol. Cell *1*, 863–872.
10. Schmucker, D., Jackle, H., and Gaul, U. (1997). Genetic analysis of the larval optic nerve projection in Drosophila. Development *124*, 937–948.
11. Bodmer, R., and Jan, Y.N. (1987). Morphological differentiation of the embryonic peripheral neurons in Drosophila. Rouxs Arch. Dev. Biol. *196*, 69–77.
12. Gao, F.B., Brenman, J.E., Jan, L.Y., and Jan, Y.N. (1999). Genes regulating dendritic outgrowth, branching, and routing in Drosophila. Genes Dev. *13*, 2549–2561.
13. Moore, A.W., Jan, L.Y., and Jan, Y.N. (2002). hamlet, a binary genetic switch between single- and multiple-dendrite neuron morphology. Science *297*, 1355–1358.
14. Brenman, J.E., Gao, F.B., Jan, L.Y., and Jan, Y.N. (2001). Sequoia, a tramtrack-related zinc finger protein, functions as a pan-neural regulator for dendrite and axon morphogenesis in Drosophila. Dev. Cell *1*, 667–677.
15. Grueber, W.B., Jan, L.Y., and Jan, Y.N. (2002). Tiling of the Drosophila epidermis by multidendritic sensory neurons. Development *129*, 2867–2878.
16. Grueber, W.B., Jan, L.Y., and Jan, Y.N. (2003). Different levels of the homeodomain protein Cut regulate distinct dendrite branching patterns of *Drosophila* multidendritic neurons. Cell *112*, 805–818.
17. Grueber, W.B., Ye, B., Moore, A.W., Jan, L.Y., and Jan, Y.N. (2003). Dendrites of distinct classes of *Drosophila* sensory neurons show different capacities for homotypic repulsion. Curr. Biol. *13*, 618–626.
18. Tracey, W.D., Jr., Ning, X., Klingler, M., Kramer, S.G., and Ger-

gen, J.P. (2000). Quantitative analysis of gene function in the Drosophila embryo. Genetics *154*, 273–284.
19. Van Doren, M., Williamson, A.L., and Lehmann, R. (1998). Regulation of zygotic gene expression in *Drosophila* primordial germ cells. Curr. Biol. *8*, 243–246.
20. Lee, T., and Luo, L. (1999). Mosaic analysis with a repressible cell marker for studies of gene function in neuronal morphogenesis. Neuron *22*, 451–461.
21. Sonoda, J., and Wharton, R.P. (1999). Recruitment of Nanos to hunchback mRNA by Pumilio. Genes Dev. *13*, 2704–2712.
22. Jaruzelska, J., Kotecki, M., Kusz, K., Spik, A., Firpo, M., and Reijo Pera, R.A. (2003). Conservation of a Pumilio-Nanos complex from Drosophila germ plasm to human germ cells. Dev. Genes Evol. *213*, 120–126.
23. Knowles, R.B., Sabry, J.H., Martone, M.E., Deerinck, T.J., Ellisman, M.H., Bassell, G.J., and Kosik, K.S. (1996). Translocation of RNA granules in living neurons. J. Neurosci. *16*, 7812–7820.
24. Clark, I.E., Dobi, K.C., Duchow, H.K., Vlasak, A.N., and Gavis, E.R. (2002). A common translational control mechanism functions in axial patterning and neuroendocrine signaling in Drosophila. Development *129*, 3325–3334.
25. Haraguchi, S., Tsuda, M., Kitajima, S., Sasaoka, Y., Nomura-Kitabayashid, A., Kurokawa, K., and Saga, Y. (2003). nanos1: a mouse nanos gene expressed in the central nervous system is dispensable for normal development. Mech. Dev. *120*, 721–731.
26. Tsuda, M., Sasaoka, Y., Kiso, M., Abe, K., Haraguchi, S., Kobayashi, S., and Saga, Y. (2003). Conserved role of nanos proteins in germ cell development. Science *301*, 1239–1241.
27. Spassov, D.S., and Jurecic, R. (2002). Cloning and comparative sequence analysis of PUM1 and PUM2 genes, human members of the Pumilio family of RNA-binding proteins. Gene *299*, 195–204.
28. Barker, D.D., Wang, C., Moore, J., Dickinson, L.K., and Lehmann, R. (1992). Pumilio is essential for function but not for distribution of the Drosophila abdominal determinant Nanos. Genes Dev. *6*, 2312–2326.
29. Rubin, G.M., and Spradling, A.C. (1982). Genetic transformation of Drosophila with transposable element vectors. Science *218*, 348–353.
30. Gavis, E.R., Lunsford, L., Bergsten, S.E., and Lehmann, R. (1996). A conserved 90 nucleotide element mediates translational repression of nanos RNA. Development *122*, 2791–2800.
31. Uylings, H.B., Smit, G.J., and Veltman, W.A. (1975). Ordering methods in quantitative analysis of branching structures of dendritic trees. Adv. Neurol. *12*, 347–354.
32. Berry, M., Hollingworth, T., Anderson, E.M., and Flinn, R.M. (1975). Application of network analysis to the study of the branching patterns of dendritic fields. Adv. Neurol. *12*, 217–245.